ON BOUNDARY CONDITIONS IN COMPUTATION OF CT-BASED FFR: A STUDY INTEGRATING PET PERFUSION IMAGES IN CFD

Ernest WC Lo[1], Leon Menezes[2], Ryo Torii[3]

[1] UCL EPSRC CDT for Medical Imaging; Department of Medical Physics and Biomedical engineering, University College London, Gower Street, London WC1B 6BT, UK, ernest.lo.15@ucl.ac.uk

[2] UCL Institute of Nuclear Medicine; NIHR University College London Hospitals Biomedical Research Centre, 235 Euston Road, London NW1 2BU, UK, leon.menezes@nhs.net

[3] UCL Mechanical Engineering, Torrington Place, London WC1E 7JE, r.torii@ucl.ac.uk

SUMMARY

Sensitivity of CT-based fractional flow reserve (FFR) calculation to inflow and outflow boundary conditions (BCs) was investigated. The inflow investigation focused on the impact of flow pulsatility, and the outflow investigation was on the effect of using patient-specific myocardial perfusion downstream to each coronary branch. The FFRs were computed for 12 patients with various degree of stenosis. CFD simulations using 3D patient-specific anatomical models with patient-specific inflow and outflow conditions indicated that the type of inflow BCs (steady/pulsatile) does not have a significant impact on computed FFRs. The FFRs derived from the two outflow BCs – determined from only vessel morphology and from myocardial perfusion – agreed in general but the difference is larger for severely diseased patients, potentially misleading the treatment. The sensitivity of FFR computations to BCs were shown not too high in general but there are some exceptions where extra care may need to be in place.

Key words: *CT-based computation of FFR, flow pulsatility, patient-specific outflow*

1   INTRODUCTION

Coronary artery disease (CAD) is the leading cause of death globally. For example, it is associated with 19% of deaths in Europe [1]. The most common form of CAD is myocardial ischemia caused by atherosclerotic narrowing in the epicardial vessels, i.e. stenosis. Fractional flow reserve (FFR), a risk indicator based on pressure drop across a stenosis, was proposed and proven as an effective method to assess the functional severity of a stenosis for clinical decision making how the stenosis should be treated [2]. While FFR is mostly calculated using intra-coronary pressure from invasive catheterization, an alternative approach using medical-image-based 3D anatomical models and computational fluid dynamics (CFD) has become a common method to non-invasively assess the severity [3].

Although the computational approach has become reasonably mature and now a variety of non-invasive FFR calculation methods – combining different imaging modalities [4-6] – exist, assumptions are inevitable in computational models which introduce uncertainties. Typical challenge can be found with boundary conditions. For example, in well-defined simulations where boundary conditions are known from invasive measurements, it was shown that FFR is not affected by the difference between steady and pulsatile flow conditions [7]. However, in practice, such a complete set of data is not always available. We therefore examined the impact of various inflow as well as outflow boundary conditions on computation of FFR, in practical scenarios, to shed light on the requirements for those conditions to ensure adequate model representation. In particular, we made a unique attempt to incorporate patient-specific outflow conditions by incorporating positron emission tomography (PET) images.

2 METHOD

2.1 Patients

This study included 13 lesions from 12 patients (7 male, 5 female, age: 61.7 ± 12.2 years) of various levels of angiographically determined epicardial stenosis (7 mild, 3 intermediate and 3 severe case). All patients underwent 4D CTCA for anatomical assessment and ^{82}Rb PET perfusion imaging to identify ischaemic regions in the myocardium. The study was carried out in accordance with the recommendations of the South East Research Ethics Research Committee (Aylesford, Kent, UK) with written informed consent from all subjects, in accordance with the Declaration of Helsinki.

2.2 General analysis approach

CTCA images were segmented to produce 3-D anatomical models of the aortic root and coronary arteries, which were then meshed using tetrahedral and prism elements, in the order of 10^6 elements per model, using Simpleware ScanIP (Synopsys, CA, USA). The blood flow in the anatomical models were computed using a commercial CFD package ANSYS CFX 17.0 (ANSYS, Inc. Cannonsburg, USA). The flow was assumed to be laminar and blood was modelled as homogenous and Newtonian fluid with its density and dynamic viscosity 1060 kg/m^3 and 0.004 Pa s, respectively. The vessel wall was approximated as rigid wall, where non-slip boundary conditions were applied, and cardiac-induced wall motion was not incorporated. Once the resulting pressure profiles across the stenosed branch is computed, ratio of the pressure downstream to the stenosis to that at the coronary ostium was calculated as FFR. In the pulsatile simulations, the lowest FFR – typically appears during the diastole – was taken as the value for the patient.

2.3 Inflow boundary conditions

The acquired CT was time series with one image set per every 10% of cardiac cycle, enabling segmentation of the LV cavity at multiple points over time. The aortic outflow waveform was estimated by calculating the temporal variation of the cavity volume across the cycle assuming the flow in the diastolic phase to be zero. Both pulsatile and steady flow simulations were carried out. For the steady state simulations, the patient-specific stroke volume per cardiac cycle (i.e. mean flow rate from the LV) was used as inflow condition.

2.4 Outflow boundary conditions

At the distal end of each branch in the 3D models, two types of boundary conditions were considered: morphology-based boundary condition (MBC) and perfusion-based (i.e. patient-specific) boundary condition (PBC). In either case, the actual outflow boundary conditions were given using 2-element Windkessel model where resistance and compliance are defined at each outlet (Figure 1). In MBC, a conventional approach, the downstream resistances were determined using a structured tree model [8] representing a peripheral vascular tree. In practice, the branching structure of the vasculature and diameter of each segment were defined using Murray's law and empirical branch ratio 9:6 [8]. The total resistance of the 'generated' vascular tree till the cut-off diameter of 50 μm was calculated for each outlet. Compliance parameter at each outlet was calculated by setting the time constant (=1/RC) equal to 0.063 s following the literature [9]. To model physiological diastolic-dominant flow in the left coronary tree, a typical left-ventricular pressure waveform was applied across the capacitance component of the Windkessel. The resistances for coronary outlets were then adjusted such that the total coronary flow accounts for 5% of the total aortic inflow and the aortic pressure pulse falls within the patient-specific systolic and diastolic brachial pressures (mean pressure was used in steady state simulations). Even after this, the resistance at the end still depends on the diameter of each outlet of reconstructed 3D model.

For the PBC, the resistance adjustment was done further for each outlet, such that the flow ratio between different coronary branches follow the proportion of blood perfusion around the corresponding outlets based on the PET images. To achieve this, CT and PET images were first co-registered using anatomical landmarks, and then the PET image intensities were sampled (representing perfusion in ml/100ml/min), around the anatomical model outlets using a sampling sphere of 20 mm diameter. Here, as in the MBC, the total coronary flow is assumed to be 5% of the

total aortic input but the peripheral resistances downstream to each of the branches do not depend on the terminal branch size.

Calculation of FFR requires the hyperaemic state, i.e. increased flow under administration of vasodilatory drug adenosine. Conventionally with MBC, hyperaemic state is represented by reduction of peripheral resistance to 30% of its original. We varied the resistance reduction from 30% to 90% of the original, in order to investigate the sensitivity of FFR to the degree of hyperaemia. With PBC, hyperaemic resistances were determined based on PET images acquired during adenosine administration, i.e. patient-specific hyperaemic state was incorporated with PBC. Here, resulting hyperaemic coronary flow is not 5% of the total aortic input any more.

3 RESULTS, DISCUSSION AND CONCLUSIONS

3.1 Impact of inflow boundary conditions – pulsatile vs steady

FFR values calculated pulsatile and steady inflow conditions are compared first, for randomly selected 4 patients with various degree of diseases (trivial-severe). The results are summarised in Table 1. Here, only MBC was used for the outflow. The FFRs under the two inflow conditions are generally in good agreement, i.e. FFR is nearly independent of the boundary conditions. Further investigation on the flow rates through various branches revealed that the flow rates through the stenosed branches are closely matched between the two simulation types while the difference in the healthy branch flows tend to be higher. The stenosis limits the flow in the branch and hence the influence of time-dependent variation of the flow is limited.

3.2 Impact of outflow boundary conditions – morphology-based vs perfusion-based

Knowing from the previous section that the steady flow can be used to sufficiently evaluate FFR, the results obtained with MBC and PBC for 11 vessels are compared while keeping inflow condition steady. All FFRs obtained with various boundary conditions are presented in Figure 2.

FFR range is from 0.56 (Patient 12 with MBC 30%) to 0.99 (Patients 6 and 7 with PBC). The range reflects the wide range of disease state included in the study, in reference to the standard diagnostic cut-off value of FFR (0.80). The FFR with PBC and 'the standard (i.e. 30%)' MBC are 0.86±0.11 vs 0.84±0.14 (p=0.59) and correlated well (r = 0.68). The correlation is higher for the patients with high FFR values (FFR >> 0.80), i.e. patients with relatively minor or insignificant stenosis. The PBC tends to result in FFRs that are higher than the ones with the conventional boundary condition (MBC 30%), i.e. the conventional assumption tends to overestimate the disease severity.
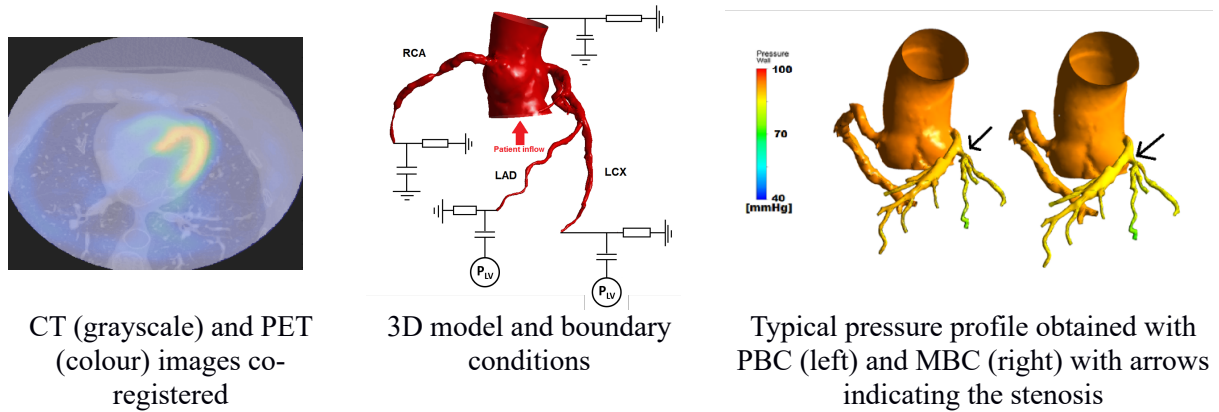
The range of FFR with the variable MBC, also shown in Figure 2, demonstrates that the variability of FFR is small (<0.03) for patients with high FFR, i.e. the less diseased patients. The range becomes much larger towards the patients with lower overall FFR, 0.22 at the maximum for LAD of Patient 12. The FFRs derived with patient-specific outflow (PBC) fell within the range of FFRs with variable MBC for most of the patients. For Patient 7 and 12 (LAD), FFR ranges are large but the entire ranges are below the 0.8 threshold, i.e. they would be in the 'diseased' category anyways.
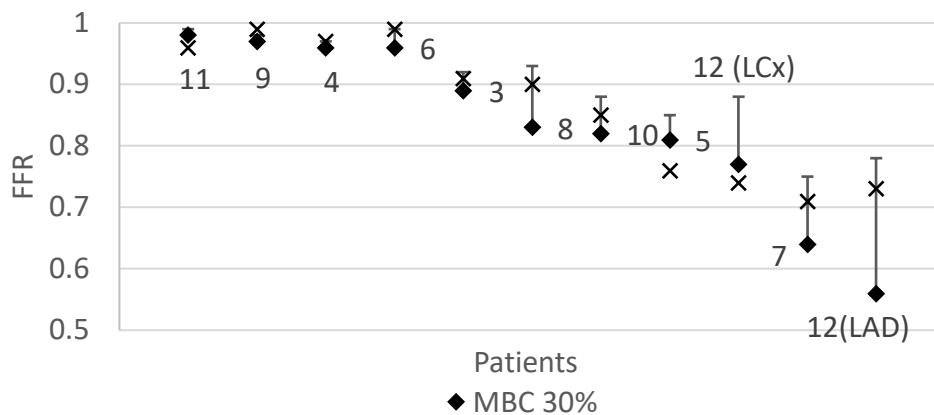
3.3 Conclusions

We conducted a series of computational FFR analysis using various inflow and outflow boundary condition to investigate their impact on the FFR derivation. The FFRs computed with the different boundary conditions agreed in general, i.e. the sensitivity of FFR computation to boundary conditions is not very high. However, the models with PET-based outflow condition revealed that there are some cases in which conventional boundary condition underestimate the functional severity of a stenosis, potentially placing the patient in different diagnostic category. The proposed method to derive a range of potential FFR for a patient, by varying peripheral resistance over a physiologically possible range, gave an additional insight into the sensitivity of FFRs. The method could potentially compensate the lack of perfusion data in analysis and may provide additional diagnostic indications.

Table 1. Comparison of FFRs obtained from two types of inflow boundary conditions.

Patient	1	2	3	4
Pulsatile FFR	0.59	0.84	0.80	0.94
Steady-MBC FFR	0.60	0.86	0.80	0.96

CT (grayscale) and PET (colour) images co-registered

3D model and boundary conditions

Typical pressure profile obtained with PBC (left) and MBC (right) with arrows indicating the stenosis

Figure 1. Analysis overview and a typical computational results.

Figure 2. The FFRs of patients ordered in reference to the value of FFR. The bars indicate the range of FFRs obtained using the various MBCs, with the conventional (MBC 30%) marked as a diamond, and the PBC marked as cross. Patient numbers are shown on the plot as reference. Patient 12 had stenosis in 2 vessels (LAD and LCx).

REFERENCES

[1] N. Townsend, L. Wilson, P. Bhatnagar, K. Wickramasinghe, M. Rayner and M. Nichols. Eur Heart J, 37(42):3232-3245, 2016.
[2] G.R. Heyndrickx and G.G. Tóth. Interv Cardiol Rev 11:116-119, 2016.
[3] A.J. Moss, M.C. Williams, D.E. Newby, E.D. Nicol. Curr Cardiovasc Imaging Rep 2017;10.
[4] C.A. Taylor, T.A. Fonte, J.K. Min. J Am Coll Cardiol 61:2233–41, 2013.
[5] Y Zhang, S. Zhang, J. Westra, D. Ding, Q. Zhao, J. Yang, Z. Sun, J. Huang, J. Pu, B. Xu, S. Tu. Int J Cardiovasc imaging, epub ahead of print, 2018.
[6] J. Ligthart, K. Masdjedi, K. Witberg, F. Mastik, L. van Zandvoort, M.E. Lemmert, J. Wilschut, R. Diletti, P. de Jaegere, F. Zijlstra, I. Kardys, N.M. Van Mieghem, J. Daemen. Circ Cardiovasc Interv 11(12):e006911, 2018.
[7] P. Siogkas and A. Papafaklis. BioMed Research International, 2015;2015:628416 (epub)
[8] M.S. Olufsen. Am J Physiol Circ Physiol 276:H257–68, 1999.
[9] H.J. Kim, I.E. Vignon-Clementel, J.S. Coogan, C.A. Figueroa, K.E. Jansen, C.A. Taylor. Ann Biomed Eng 38:3195–209, 2010.